## University of Bristol - Explore Bristol Research
### General rights

# 3D Expression Patterns of Cell Cycle Genes in the Developing Chick Wing and Comparison With Expression Patterns of Genes Implicated in Digit Specification

Monique Welten, Gordana Pavlovska, Yu Chen, Yuko Teruoka, Malcolm Fisher,[†] Fiona Bangs Matthew Towers, and Cheryll Tickle*

**Sonic hedgehog (Shh) signalling controls integrated specification of digit pattern and growth in the chick wing but downstream gene networks remain to be unravelled. We analysed 3D expression patterns of genes encoding cell cycle regulators using Optical Projection Tomography. Hierarchical clustering of spatial matrices of gene expression revealed a dorsal layer of the wing bud, in which almost all genes were expressed, and that genes encoding positive cell cycle regulators had similar expression patterns while those of *N-myc* and *CyclinD2* were distinct but closely related. We compared these patterns computationally with those of genes implicated in digit specification and *Ptch1*, 50 genes in total. Nineteen genes have similar posterior expression to *Ptch1*, including *Hoxd13*, *Sall1*, *Hoxd11*, and *Bmp2*, all likely Gli targets in mouse limb, and cell cycle genes, *N-myc*, *CyclinD2*. We suggest that these genes contribute to a network integrating digit specification and growth in response to Shh. *Developmental Dynamics 240:1278–1288, 2011*. © 2011 Wiley-Liss, Inc.**

## INTRODUCTION

The chick wing is a major model for investigating mechanisms involved in pattern formation in vertebrate embryos with specification of digit pattern being integrated with growth (Towers et al., 2008). The three digits arise from the posterior part of the wing bud (Vargesson et al., 1997) and are arranged in the pattern 2,3,4 (running from anterior to posterior; in the hand, the antero-posterior axis runs from thumb to little finger).

Digit pattern formation is controlled by signaling of the polarizing region, a small group of mesenchyme cells at the posterior margin of the wing bud (Saunders and Gasseling, 1968). When the polarizing region from one wing bud is grafted to the anterior margin of a second bud, six digits form with an additional set of digits developing in mirror image symmetry with the normal set giving the pattern 432234. It was proposed that the polarizing region produces a diffusible morphogen that sets up a concentration gradient in cells adjacent to the polarizing region, the local morphogen concentration providing cells with positional information and cells then using this information to form the appropriate digit (Wolpert, 1969). It was also shown that polarizing region grafts induce cell proliferation in responding cells (Cooke and Summerbell, 1980).

John Fallon was one of the embryologists who carried out early studies on the polarizing region, showing, for

example, that limb buds of other vertebrates had a polarizing region that could induce additional digits when transplanted to the chick wing bud (Fallon and Crosby, 1977). However, at that time, there was complete ignorance about molecules involved in digit patterning and nature of postulated morphogen and growth controlling factor(s) produced by the polarizing region. It is now known that the polarizing region expresses *Shh*, which encodes a secreted molecule (Riddle et al., 1993) and it is well established that Shh is pivotal in digit patterning. We have also recently shown that Shh signaling controls growth of the digit-forming region of the wing bud (Towers et al., 2008). Therefore, identifying genes downstream of Shh signalling in limb should provide information about the gene networks involved in both patterning and growth.

Considerable progress has been made in unravelling how Shh signals are transduced. The transcriptional effectors of Shh signalling are Gli proteins; in the absence of Shh, Gli2 and Gli3 proteins are processed into forms that act as repressors, while in the presence of Shh, Gli1, Gli2, and Gli3 proteins function as activators. Shh signaling is pivotal in digit patterning, mainly acting by relieving repression of target genes by Gli3 in the posterior digit-forming region of the limb bud (Litingtung et al., 2002; te Welscher et al., 2002). Relatively little is known, however, about the target genes in the limb bud whose expression is either activated or de-repressed in response to Shh signalling.

Several transcription factors have been implicated in digit patterning including *Hoxd13, Tbx2, Tbx3, Sall1* (reviewed in Tickle, 2006) and recently Vokes and colleagues (Vokes et al., 2008) identified *Hoxd13* and *Sall1* as direct Gli targets in the mouse limb. *Hoxd13* is expressed in the posterior region of both chick and mouse limbs due to the relief of Gli3 repression by Shh signalling (Litingtung et al., 2002, te Welscher et al., 2002). We also identified a set of genes in the chick wing that are likely to be expressed downstream of Shh signalling and whose expression is regulated in the same way as *Hoxd13* using microarray analysis of tissues

from both normal and *talpid³* chicken mutant wing buds (Bangs et al., 2010). Both Gli activator and Gli repressor functions fail in *talpid³* cells due to lack of primary cilia (Yin et al., 2009) and in *talpid³* wing buds, *Hoxd13* is ectopically expressed in the anterior region due to failure of Gli3 repression. With respect to genes involved in growth downstream of Shh signalling in the chick wing, we have shown experimentally that expression of genes encoding the cell cycle regulators, *N-myc* and *Cyclin D*, depends on Shh signalling (Towers et al., 2008). We have also described whole mount in situ hybridization expression patterns of E2F transcription factors in developing chick wing (Towers et al., 2009) but how expression of these cell cycle genes is regulated is not known.

In order to compare multiple patterns of gene expression in the developing chick wing and thus identify genes that are expressed in similar spatial patterns and likely to be regulated in the same way and/or may be functionally related, we have visualized 3D expression patterns using Optical Projection Tomography (OPT; Sharpe et al., 2002) and then analyzed the digital data computationally (Fisher et al., 2008; Bangs et al., 2010). Expression patterns are accumulated onto a digitized reference wing bud, which is then subdivided into spatial domains and the levels of expression of each gene in all these domains throughout the wing bud can be computed. Hierarchical clustering of the data can be used to reveal clusters of spatial domains of gene expression, thus dividing the wing bud into mutually exclusive regions with unique gene transcriptional signatures, and to reveal clusters of mutually exclusive groups of genes that are expressed in similar patterns, groups of syn-expressed genes. It should be noted, however, that genes can be expressed in more than one spatial domain cluster.

Here we have mapped 3D expression of 12 cell cycle genes in stage-24 chick wing buds and identified unique spatial domains of expression and groups of syn-expressed genes. We then compared the 3D expression patterns of these cell cycle genes with those of genes implicated in digit

specification (mostly data from Bangs et al., 2010) and *Tbx2, Tbx3*, and *Sall3* (Fisher et al., 2011). We also included in the analysis the 3D pattern of expression of *Ptch1*, which reports cells responding to Shh, and *Shh* itself. Hierarchical clustering was then carried out on all the 3D mapped data, a total of 50 gene expression patterns (see Supp. Fig. S1, which is available online, for details of the 50 genes mapped and used for computational analysis). We were then able to identify unique spatial domains of gene expression within the wing bud in which both cell cycle and "patterning" genes are expressed and also groups of syn-expressed cell cycle and "patterning" genes that could represent the network that integrates growth and digit specification. The addition of *Ptch1* to the analysis also provides a way of confirming that expression of the genes identified is likely to be downstream of Shh signalling.

## RESULTS

### Cell Cycle Genes

3D expression patterns of 12 cell cycle genes (*CyclinD1, D2*, and *D3, E2F1,2,3,5,7,8, C-myc, N-myc, PCNA*) were visualized in stage-24 chick wing buds following whole mount in situ hybridization using OPT. *PCNA* gene expression is a marker for proliferating cells (Kohler et al., 2005). Expression patterns obtained in this series of experiments generally matched those previously reported.

Figure 1 shows representative 3D expression data for *PCNA, N-myc, CyclinD2*, and *E2F8*. *PCNA* transcripts are abundant throughout most of the wing bud except the proximal central region (near base of wing bud) indicating that proliferation is widespread (Fig. 1A, B). Figure 1C illustrates *PCNA* expression mapped on to stage-24 reference wing bud visualised using the Amira isosurface feature. The region of weaker expression can be seen more clearly using a color-mapped volume rendering (Amira voltex feature) that produces a heat map (Fig. 1D). In contrast to the almost ubiquitous expression of *PCNA*, expression of *N-myc* and *Cyclin D2* is more distally and
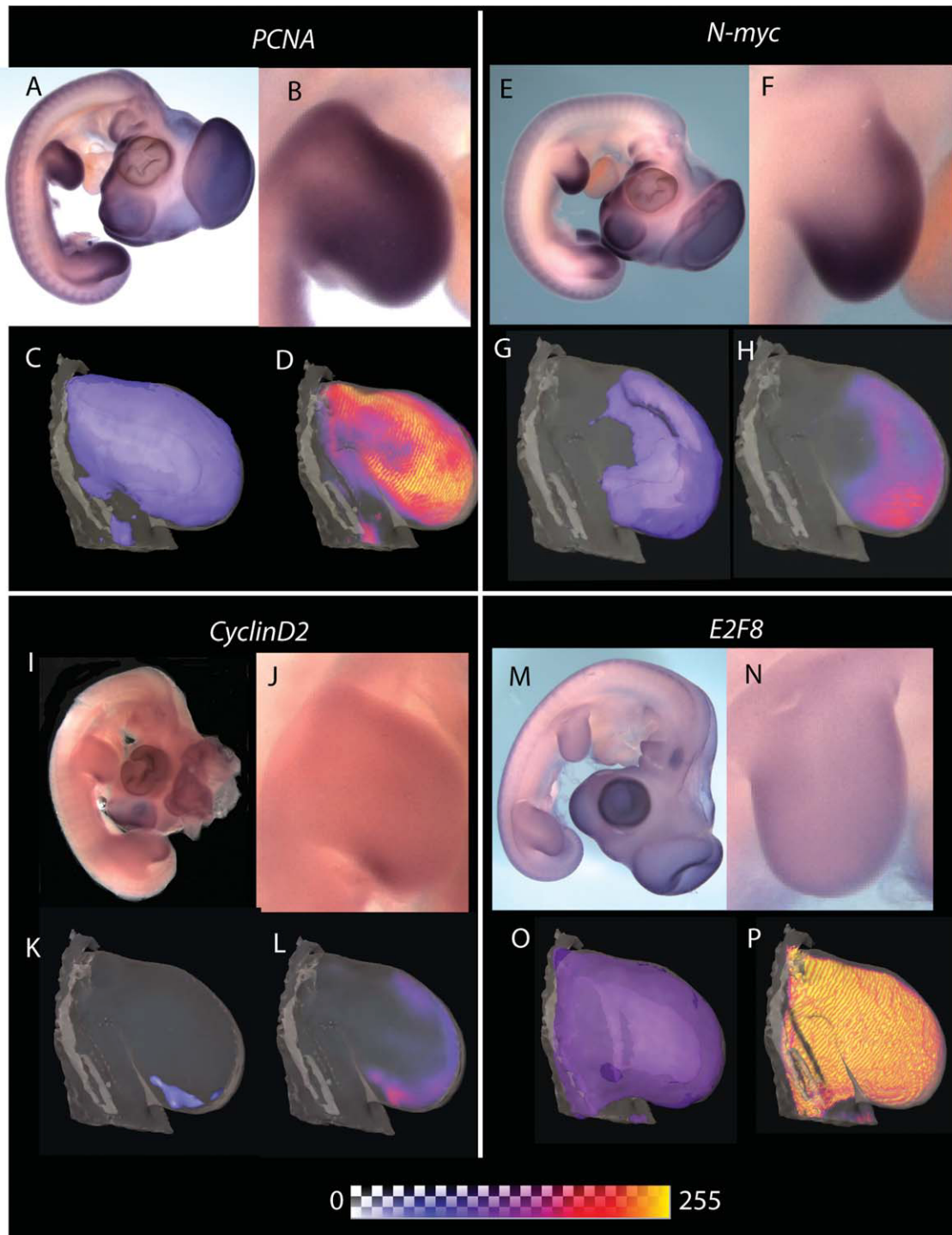
**Fig. 1.** 3D cell cycle gene expression patterns in stage-24 chick wing bud. Whole mount in situ hybridization patterns and 3D representations of 4 genes from the cell cycle dataset: *PCNA* (A–D), *N-myc* (E–H), *CyclinD2* (I–L) and *E2F8* (M–P) at stage 24. **A,E,I,M**: Whole mounts of embryos. **B,F,J,N**: High-power images of right wing buds. **C,G,K,O**: Surface rendering of the gene expression patterns warped on to the reference wing. **D,H,L,P**: Volume rendering of gene expression pattern in C,G,K,O showing levels of expression indicated by heat map; see bar below. Anterior is up, posterior is down. Note *PCNA* and *E2F8* widely expressed whereas *N-myc* and *CyclinD2* expressed at high levels distally and posteriorly.

posteriorly restricted. *N-myc* is expressed at higher levels at the posterior distal tip of the wing bud (Fig. 1E–H) while *CyclinD2* is expressed in an even more restricted posterior-distal pattern (Fig. 1I–L). On the other hand, *E2F8* is expressed at high levels throughout the wing bud (Fig. 1M–P). Note that whole mount in situ hybridization in this case was performed using half the concentration of NBT and this is why the signal

appears faint (Fig. 1 M, N). Whole mount in situ hybridization data for all the other cell cycle genes and all the 3D expression patterns can be viewed at https://www.echickatlas.org/submission/login (username GUEST, password guest).

3D expression data for the 12 genes (3 replicates for each) were mapped onto the stage-24 reference wing bud and the median for each gene was derived. The reference limb with mapped median expression patterns was then divided into 2,072 spatial domains, from hereon referred to as tiles, using MRC HGU software. Expression levels of each gene in all the different tiles were computed. These data were then tabulated in a tab-delimited file to generate a matrix of gene expression across all tiles. A hierarchical clustering method (Pearson Correlation) was applied to the tiles to cluster spatial domains of gene expression; gene expression data were clustered to define gene synexpression groups.

Hierarchical clustering of the spatial domains of gene expression generated 19 clusters (Fig. 2 A, B, see Supp. Fig. S2, which is available online). *PCNA* is expressed at high levels (at levels > 50 greyscale units) in 50% of the tiles in the stage-24 wing bud. Four spatial domain clusters (13, 15, 18, 19) in which *PCNA* is expressed are shown in Figure 2A, 3D representations in Figure 2B. All 12 genes except *E2F7* are expressed in a dorsal layer of the wing bud (cluster18; see Supp. Movie S1, see also Fig. 3). All 12 genes except *E2F7* are also expressed more medially and ventrally (cluster19) but at different levels (see Supp. Movie S1). For example, *E2F1* and *E2F2* are expressed in 70% of tiles in cluster 18 (at levels > 50 greyscale units) but in 48% of tiles in cluster 19. All cell cycle genes except *E2F7, CyclinD2*, and *N-myc* are expressed in a smaller medial domain (cluster15) and *CyclinD3, E2F5*, and *E2F8* are expressed at high levels in a domain that includes posterior bud tip (cluster 13; Fig. 2B).

Hierarchial clustering of the genes resulted in 6 gene clusters, as defined by terminal nodes (ends of dark blue lines, Fig. 2C). The largest cluster represents a group of 5 syn-expressed genes (yellow); *PCNA* and 4 cell cycle

genes, *E2F1, E2F2, E2F3*, and *C-myc*, which all encode positive regulators of S phase entry. *E2F7*, encoding a negative regulator, is on its own. *N-myc* and *CyclinD2* expression patterns although treeing out separately are closely related. *CyclinD1* is also on its own while *CyclinD3, E2F5*, and *E2F8* cluster together.

We also determined 3D expression patterns of cell cycle genes at stages 21 and 27 (Fig. 3). *E2F6*, included for stage 27, is expressed in medial region of wing bud. Comparison of patterns at stages 21 and 27 using the same computational analysis as above revealed an extensive dorsal domain (Fig. 3A–C), similar to that seen at stage 24, in which all the genes except E2F7 were expressed. With respect to gene syn-expression groups, *PCNA* clusters with genes encoding positive cell cycle regulators at both these stages as it did at stage 24 (yellow boxes, Fig. 3D), with *E2F1* and *C-myc* clustering with PCNA (purple lettering) at all 3 stages. *N-myc* and *CyclinD2* are nearest neighbours at stage 27 just as they are at stage 24 (Fig. 3D).

## Comparison of 3D Expression Patterns of Cell Cycle Genes and Genes in *Hoxd13* Microarray Cluster and Other Genes Implicated in Digit Patterning

Median 3D expression patterns of the cell cycle regulatory genes, genes of the *Hoxd13* microarray cluster, including those in Bangs et al. (2010), *Tbx2, Tbx3, Sall3, Shh*, and *Ptch1*, a total of 50 gene expression patterns, were accumulated onto a digitized stage-24 reference wing bud. Whole mount in situ hybridization patterns of *Angpt2, Bmp2, Hoxa9, Hoxd11, Hoxd12, Snai2, Wnt5a, Ptch1*, and *Notum* in stage-24 chick wing buds are shown in Supp. Figure S3. These patterns and those for other genes in this study, including 3D expression data, can be viewed at https://www.echickatlas.org/ submission/login (username GUEST, password guest). Spatial levels of expression of each gene throughout the wing bud were computed and the data were then hierarchically clustered.

Twenty-four clusters of spatial domains were produced. Different views of a sub-set of these spatial domain clusters are shown in Figure 4 and in Supp. Movie S2.

One medially located spatial domain, cluster 21, contains 44 out of 50 genes (*MME, Notum, Wnt5a, Angpt2, Shh*, and *E2F7* not expressed) while another large domain, cluster 24 (Fig. 4Aiii, 4B iii, 4C iii) at the distal rim of the wing bud also contains 44/50 genes but has a different transcriptional signature (*AGPAT, FAM123a, FSTL4, Notum, MME*, and *E2F7* not expressed). Both of these clusters include expression of *Hoxd13, Ptch1, PCNA* and all the cell cycle genes except *E2F7* while *Shh* is expressed only in the spatial domains in cluster 24. Thirty-three of fifty genes are expressed in another large dorsal domain cluster (cluster 16), including *PCNA* and all the cell cycle genes (except *E2F7*), *Ptch1, Hoxd12, Tbx2, Tbx3*, and *Sall3* but not *Hoxd13, Shh*, and *Notum* which are very posteriorly restricted. When the number of spatial clusters is increased, the distal cluster 24 breaks up into 4 sub-clusters, which include a compact posterior cluster (sub-cluster 24a) in which 42 out of 50 genes are expressed including *Tbx2, Tbx3*, and *Sall3* (*AGPAT, FAM123, FSTL4, MME, Notum, SMYD, Hoxd12, E2F7* not expressed).

Eight gene clusters were produced from the 3D expression data from the 50 genes. A large cluster of genes that are in a syn-expression group with *Hoxd13* (mauve; 19 genes in all) includes not only genes like *Sall1*, already implicated as a Gli target in the mouse limb (Vokes et al., 2008) and in digit pattern specification, together with the related *Sall3* gene, but also the cell cycle genes *CyclinD2* and *N-myc* (Fig. 4D). When the number of gene clusters is increased, this cluster breaks down into 3 sub-groups and *Hoxd13* clusters only with *Angpt2*. Another large syn-expression group (yellow) contains *PCNA* and all the rest of the cell cycle genes except *E2F7* and *Hoxa11*. *Tbx2* and *Tbx3* cluster together separately as expected because they are expressed in both anterior and posterior stripes in the chick wing (Isaac et al., 1998).
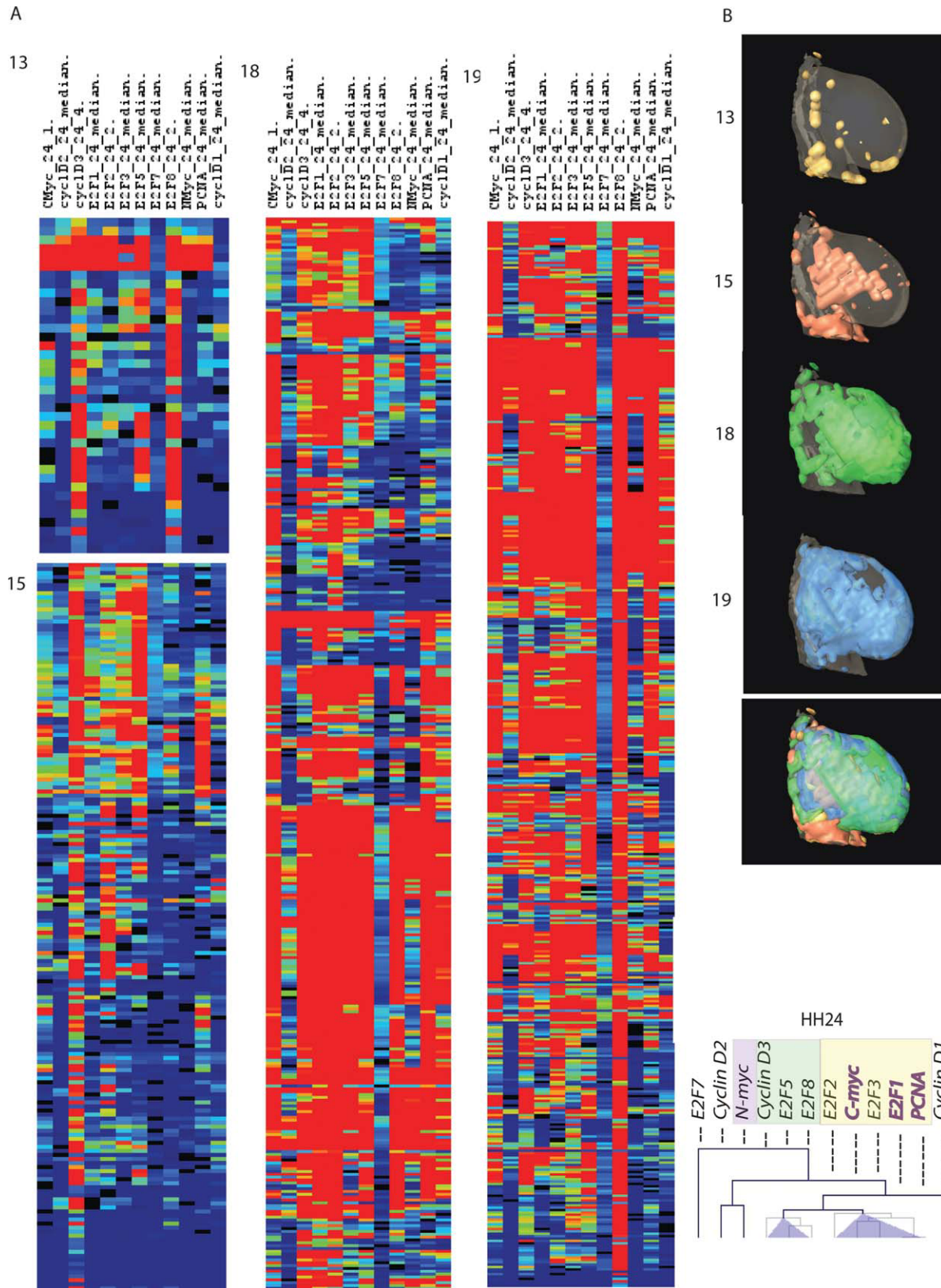
**Fig. 2.**    Comparison of 3D cell cycle gene expression patterns in stage-24 chick wing bud. Hierarchical clustering of median 3D expression patterns of cell cycle genes. **A**: Matrices showing clusters of median 3D expression patterns generated using 12 cell cycle genes. Each cell represents a 5 × 5 × 5 voxel spatial volume in stage-24 reference limb coloured according to mean signal intensity. Red = high gene expression to dark blue = low expression. Columns, genes; rows, spatial domains. Only a subset of unique spatial domain clusters, 13, 15, 18, and 19, in which *PCNA* is expressed, is shown, the remaining spatial domain clusters in Supp. Figure S2. **B**: 3D visualizations of spatial domain clusters in A together with composite visualization of all 4 domains (bottom panel). **C**: Gene clustering of median 3D expression data for 12 cell cycle genes. Six gene syn-expression groups at terminal nodes (indicated by ends of dark blue lines); each syn-expression group indicated by coloured box.

Developmental Dynamics
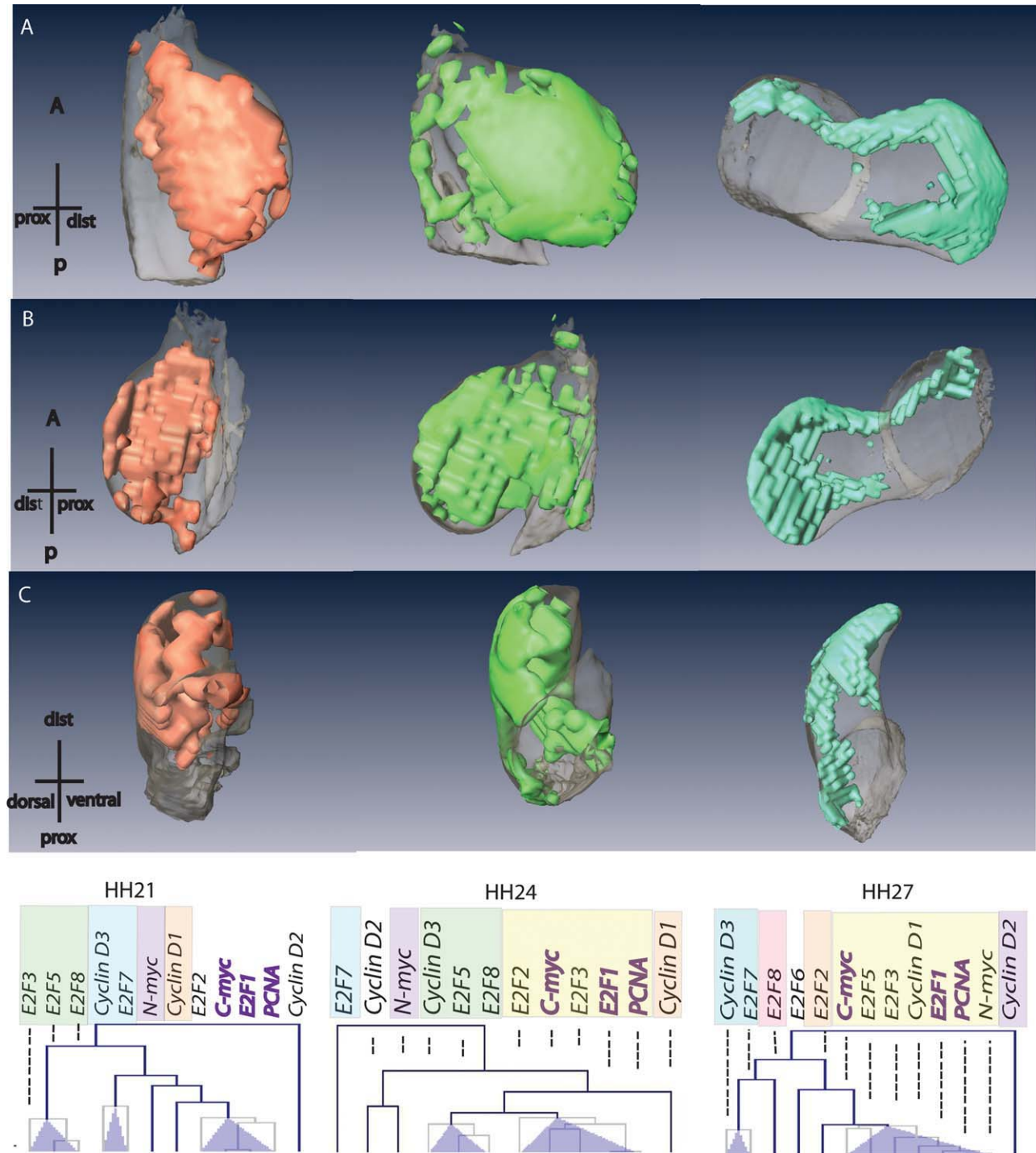


**Fig. 3.** Comparison of 3D cell cycle gene expression patterns in stage-21, -24, and -27 chick wing buds. Large dorsal spatial domain cluster and gene clusters produced by hierarchial clustering of median 3D expression patterns generated using 12 cell cycle genes at stage 21 and 24 and 13 genes at stage 27. **A–C**: 3D visualizations dorsal spatial domains at the 3 stages shown from different angles, orientation of right wing bud models indicated at left of diagram. A, anterior; P, posterior; prox, proximal; dist, distal. **D**: Gene clustering of median 3D expression data for cell cycle genes at stages 21, 24, and 27. Six synexpression groups; each syn-expression group indicated by coloured box. Genes that appear together in same syn-expression group over the 3 different stages highlighted in purple.

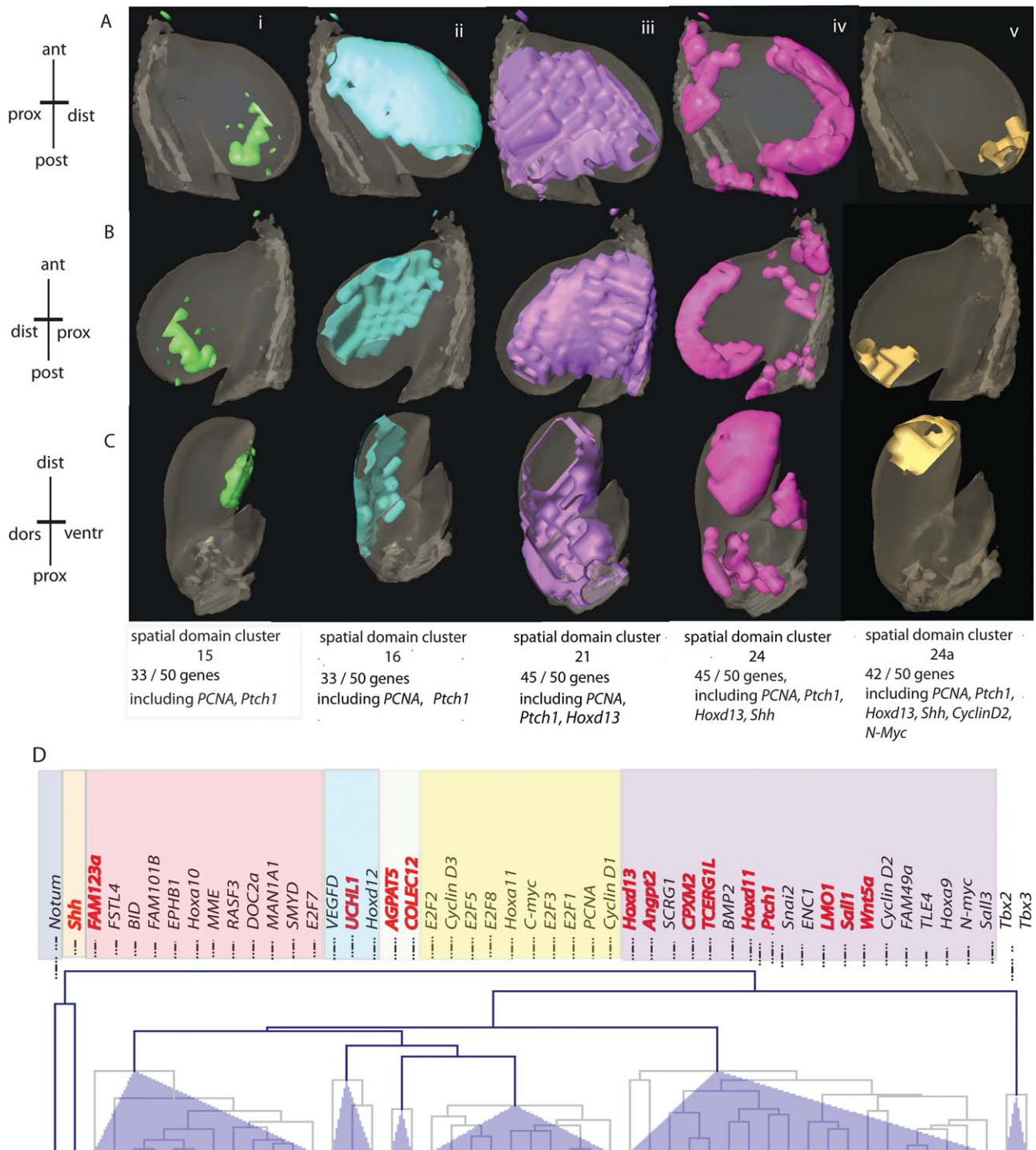**Fig. 4.** Comparison of 3D patterns of cell cycle gene expression and expression of genes implicated in digit patterning in stage-24 chick wing bud. Unique spatial domain clusters and gene clusters produced by hierarchical clustering of median 3D expression patterns generated using all 50 genes. **A–C**: Four spatial domain clusters in which both *Ptch1* and *PCNA* are expressed shown at different angles, orientation of right wing bud model indicated at left of diagram. ant, anterior; post, posterior; prox, proximal; dist, distal; dors, dorsal; ventr, ventral; i, spatial domain cluster 15; ii, cluster 16; iii, cluster 21; iv, cluster 24; v, sub-cluster 24a. Details of other genes expressed in the domains in boxes below. Note 45 genes including *PCNA, Ptch1, Hoxd13*, and *Shh*, expressed in spatial domain cluster 24 stretching along wing bud rim. When spatial domain cluster 24 is divided into 4 sub-clusters, one posterior domain cluster, 24a (right-hand image) still contains expression of 42 genes including *PCNA, Ptch1, Hoxd13, Shh, N*-myc and *CyclinD2*. **D**: Gene clustering of median 3D expression data for 50 genes. Eight syn-expression groups; syn-expression group containing *Hoxd13* highlighted in purple, syn-expression group containing PCNA highlighted in yellow. Genes in red highly expressed in *Ptch1* domain and not elsewhere in wing bud (points on y axis in Fig. 5D).

## Identification of Genes Expressed in Cells Responding to Shh

*Ptch1* expression is a reporter for cells responding to Shh signalling and *Ptch1* is in the *Hoxd13* syn-expression group (Fig. 4D) consistent with genes in this group being downstream of Shh signalling. In order to investigate more directly the relationship between *Ptch1* expression and expression of all the other genes in the dataset, we identified the tiles in the wing bud in which *Ptch1* is highly expressed (>50 greyscale units; 97 tiles; this represents the *Ptch1* spatial domain Fig. 5A) and then looked for genes also highly expressed (>50 greyscale units) in the same tiles but not highly expressed in the remaining 1,975 tiles. Figure 5B shows a scatter plot with percentage of tiles within the *Ptch1* domain in which a gene is highly expressed along the y axis and percentage of tiles in the rest of the wing bud in which a gene is highly expressed along the x axis. Genes in the *Hoxd13* syn-expression group including *N-myc* and *CyclinD2* (yellow) are highly expressed in tiles within the *Ptch1* domain but generally only in relatively few tiles outside the domain. Indeed, 8 of these genes *CPXM2, Hoxd13, LMO1, TCERG1L, Sall1, Wnt5a, Angpt2,* and *Hoxd11* are on the y axis (i.e., not highly expressed in any tiles outside the *Ptch1* domain; underlined) together with 4 other genes *AGPAT5, COLEC12, UCHL1,* and *FAM123a,* which are not in the *Hoxd13* syn-expression group. *Shh* expression lies entirely within the *Ptch1* domain as expected. All genes on the y axis are shown in red in Figure 4D. According to this analysis, the gene whose high level expression pattern is closest to that of *Ptch1* is *N-myc.* Other cell cycle genes (yellow) group together and are expressed at high levels in the *Ptch1* domain but also elsewhere in the wing bud.

## DISCUSSION

We have analysed 3D expression patterns of 12 cell cycle genes in the developing chick wing. Hierarchical clustering of the 3D data highlighted a dorsal layer of the wing bud, in
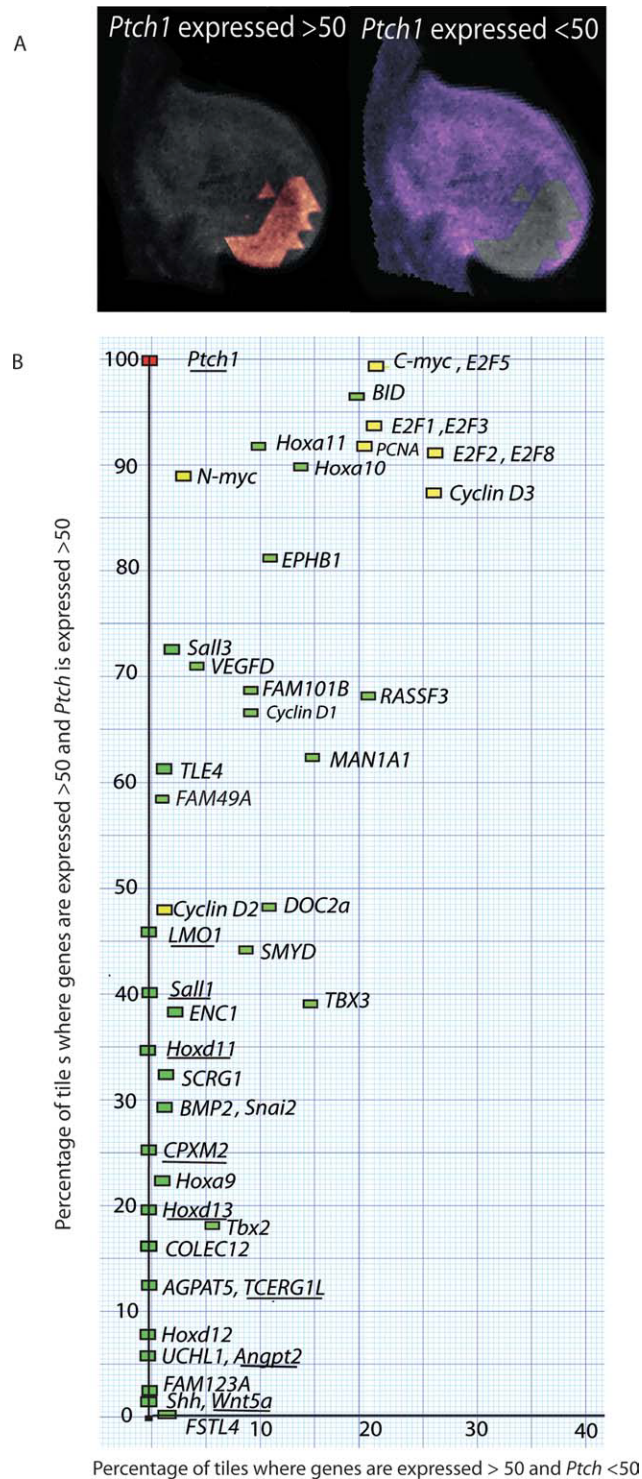


**Fig. 5.** Genes expressed in the region of the stage-24 chick wing bud where *Ptch1* is expressed at high levels. **A**: Diagram illustrating domain of 97 tiles where *Ptch1* is expressed at high levels (>50 greyscale units) in the wing bud (orange on left) and complementary domain where *Ptch1* is not highly expressed (purple on right; 1,975 tiles). **B**: Scatter plot of gene expression data. Y axis: Percentage of 97 tiles where genes expressed >50 and where *Ptch1* is expressed >50; X axis: percentage of 1,975 tiles where genes expressed >50 and where *Ptch1* is expressed <50. Plot reveals that high level expression of genes in the *Hoxd13* cluster (underlined) is not found outside *Ptch1* domain (i.e., points are close to Y axis) although the percentage of tiles in which genes are expressed within the domain can vary considerably from >10% (e.g., *Wnt5a*) to around 90% (*N-myc*). Note that *N-myc* and *CyclinD2* (yellow) are much closer to the Y axis than other cell cycle genes (yellow), which form a distinct cluster of genes highly expressed throughout *Ptch1* domain but also elsewhere in wing bud.

which all cell cycle genes except *E2F7* were expressed at stages 21, 24, and 27. Preferential growth of the wing bud dorsally could be important in producing the ventral curling of the bud. This elevated dorsal expression of cell cycle genes was not previously appreciated and demonstrates how 3D analysis can highlight dorso-ventral differences in expression. It seems likely that expression of the cell cycle genes in this syn-expression group could be regulated in the same way, by Wnt and FGF signals from the dorsal ectoderm and/or from the apical ectodermal ridge, respectively. In addition to finding clusters of spatial domains of gene expression, we also identified clusters of syn-expressed cell cycle genes. Positive regulators of the cell cycle tend to be similarly expressed with *PCNA, E2F1,* and *C-myc* having similar expression patterns across all three stages together with *E2F3* at later stages (both *E2F1* and *E2F3* encode positive regulators of the G1/S transition). *E2F7* encodes an inhibitor of G2/M transition and is very weakly expressed throughout the wing bud. Expression patterns of *N-myc* and CyclinD2, also encoding positive regulators of the G1/S transition, are distinct but closely related.

When we compared 3D expression patterns of these cell cycle genes and genes identified by microarray analysis as being downstream of Shh signalling and/or implicated in digit patterning, most genes, including cell cycle genes (except E2F7), were expressed at the very posterior wing bud tip overlapping with *Shh* and *Ptch1* expression, but many of these, particularly cell cycle genes, were also expressed more widely. We also identified a gene syn-expression group comprising 19 posteriorly expressed genes; *Hoxd13,* most of the genes in the *Hoxd13* cluster previously found to be in the same syn-expression group as *Hoxd13* (Bangs et al., 2010), other genes implicated in digit patterning, and the cell cycle genes, *N-myc* and *CyclinD2.* This group also included *Ptch1*, and direct comparison between *Ptch1* and expression of the other 49 genes confirmed that the 19 genes in the *Hoxd13* syn-expression group together with a few other genes are

highly expressed specifically in cells responding to Shh. We suggest that genes in this group contribute to a network integrating digit patterning and growth in the wing downstream of Shh signalling.

*N-myc* and *CyclinD2,* the two cell cycle genes in the *Hoxd13* syn-expression group, may play a specific role in mediating growth of the digit-forming field required for proper digit patterning. *CyclinD2* expression is directly regulated by N-myc (Bouchard et al., 1999) and, in posterior wing bud, is very sensitive to inhibition of Shh signaling by cyclopamine. Like other genes in the syn-expression group, *N-myc* and *CyclinD2* are expressed throughout the distal region of *talpid³* chicken mutant wing buds (Towers et al., 2008) suggesting that expression in normal wing buds is restricted posteriorly due to Gli3 repression anteriorly. Thus the dramatic increase in growth in *talpid³* chicken mutant wing buds is due to lack of Gli3 repressor function. Although Gli binding sites have been identified in promoters of both *N-myc* and *CyclinD2* human genes (Katoh and Katoh, 2009), these genes were not identified as being direct Gli targets in mouse limb (Vokes et al., 2008). Failure to identify these cell cycle genes in the mouse could be due to the fact that the limbs were analysed at a later stage in development.

Five genes in the *Hoxd13* syn-expression group found here have already been shown to be likely Gli targets in the mouse with *Hoxd13, Hoxd11* and *Sall1* being regulated by Gli3 repressor and and *Bmp2* by Gli activator (Vokes et al., 2008; Fig. 5, Table S6). However, *Bmp2* is expressed throughout the distal region of *talpid³* chicken mutant wing buds (Francis-West et al., 1995) and is also extended anteriorly in limb buds of *Gli3−/−* and *Gli3−/− Shh−/−* mouse embryos (Litingtung et al., 2002) suggesting regulation via Gli3 repression.

Other genes found to be syn-expressed with *Hoxd13* include *Snai2* (formerly known as *Slug*) and *Wnt5a. Snai2* encodes a member of the Snail family of zinc finger transcription factors (Nieto, 2002). Microarray analysis of mouse limbs also identified *Snail* as a gene preferentially expressed posteriorly but no Gli-binding

sites were detected in the mouse gene promoter suggesting that *Snail* is an indirect target of Shh signalling (Table S6, Vokes et al., 2008). *Snai2* has been suggested to be involved in chick wing outgrowth (Ros et al., 1997; Buxton et al., 1997) but has a better known role in chick neural crest cell migration and epithelial-mesenchymal transition, which involves changes in cell polarity (Nieto, 2002). Interestingly, *Wnt5a* has recently been suggested to act as a chemotactic factor for cells in the limb bud and thus play a role in outgrowth (Wyngaarden et al., 2010). Our analysis suggests that expression of these two genes may be regulated by Shh signalling, perhaps indicating another aspect of the way in which patterning and growth are integrated in the developing limb.

## EXPERIMENTAL PROCEDURES

### Embryo Preparation

Fertilized White Leghorn chick eggs were incubated in a humidified incubator at 38°C until embryos were at a desired developmental stage (Hamburger and Hamilton stages 21, 24, and 27; Hamburger and Hamilton, 1951). Embryos were removed to ice-cold Phosphate Buffered Saline (PBS; 0.02 M phosphate, 0.15 M NaCl) and cleaned of extra-embryonic membranes. Eyes and forebrain were punctured with a tungsten needle to reduce trapping of riboprobe and hearts punctured to allow escape of blood, which would give a false signal due to auto-flourescence.. Embryos were transferred to 4% ice-cold para-formaldehyde (PFA) overnight, then put through graded methanol series at 4°C; ending in 2 × 100% methanol washes, stored at −20°C and used within 6 weeks.

### Probe Synthesis and In Situ Hybridization

Probes were synthesized using a standard method and in situ hybridization was carried out using a protocol adapted from Nieto et al. (1993) (http://www.echickatlas.org/submission/protocols).

For E2F cell cycle genes, embryo staining with NBT/BCIP was carried out using half the normal concentration of NBT (http://www.echickatlas.org/submission/protocols/show/10) for scanning with a Bioptonics 3001 OPT scanner. (A Bioptonics Scanner has a stronger UV lamp than the prototype scanner, causing excess NBT/BCIP to develop background color and interfere with the gene expression signal.) After in situ hybridization, embryos were embedded in 1% low melting point agarose, dehydrated in Methanol, and cleared in Benzyl Alcohol – Benzyl Benzoate for subsequent Optical Projection Tomography (OPT; Sharpe et al., 2002).

## OPT Scanning

OPT scanning was carried out using either a Bioptonics 3001 scanner (www.bioptonics.com) or a prototype OPT scanner. A GFP channel was used to scan the outline and anatomy of embryos, a bright-field channel was used to visualize gene expression patterns. Resulting bitmap stacks (Bioptonics) and wlz objects (prototype scanner) (http://genex.hgu.mrc.ac.uk/Software/woolz/) were imported into Amira 5.2 software (http://www.amira.com/) and surface renderings of embryo and volume renderings of gene expression pattern generated using isosurface and voltex features, respectively. Surface renderings used for warping and volume renderings produced heat maps indicating levels of expression.

## Mapping and Computational Analysis

Mapping of 3D gene expression data on to reference models of stage-21, -24, and -27 chick wing buds was performed using Amira 5.2 software. Right wing buds were electronically cropped from samples and data to be mapped were first roughly aligned with the reference model, then, corresponding sets of landmarks, based on prominent morphological features of the wing bud, were set up between the reference wing bud and the anatomical surface of the sample. These data were then warped using a Bookstein thin plate spline method provided by Amira. The same warp was then applied to gene expression data for that sample wing. For all 50 genes, 3 duplicates were warped onto the same stage-24 reference wing. Three duplicates of cell cycle genes were also warped on to the same reference wings at stage 21 and 27. Mapped gene expression data were then converted to wlz objects (website), which hold mapped gene-expression data as a grey-level image, from 0–255 shades of grey (on an 8-bit greyscale), where 0 is black/no gene expression signal and 255 is white/high gene expression signal. Mapped data were processed with in-house software to derive a median expression pattern for each gene (MRC HGU, Edinburgh, http://genex.hgu.mrc.ac.uk/MouseAtlasCD/html/guides/WlzUtilities). Each reference wing with the median mapped data was then divided into tiles (i.e., unique spatial domains measuring $5 \times 5 \times 5$ voxels); 923 tiles for stage 21, 2,071 for stage 24 and 4,444 for stage 27. For each tile, mean signal intensity values of each gene expression pattern were calculated using in-house software (MRC HGU, Edinburgh) (Fisher et al., 2008; Bangs et al., 2010). These data were organized in a tab-delimited file that can be imported into TMeV (http://www.tm4.org/mev/) software, where they can be visualised in a 2D matrix and analyzed using hierarchical clustering algorithms. Hierarchical clustering using Pearson Correlation was applied to gene expression data to produce trees showing clusters of genes; and to the tiles to produce trees showing clusters of spatial domains of gene expression. Clusters of spatial domains of gene expression were imported into Amira to produce 3D visualizations. The tab-delimited file can be processed with EXCEL to calculate percentage of tiles in a spatial domain in which expression of a gene is >50 on an 8-bit greyscale.

## ACKNOWLEDGMENTS

## REFERENCES

Bangs F, Welten M, Davey MG, Fisher M, Yin Y, Downie H, Paton B, Baldock R, Burt DW, Tickle E. 2010. Identification of genes downstream of the Shh signalling in the developing chick wing and syn-expressed with Hoxd13 using microarray and 3D computational analysis. Mech Dev 127:428–441.

Bouchard C, Thieke K, Maier A, Saffrich R, Hanley-Hyde J, Ansorge W, Reed S, Sicinski P, Bartek J, Eilers M. 1999. Direct induction of cyclin D2 by Myc contributes to cell cycle progression and sequestration of p27. EMBO J 18:5321–5333.

Buxton P, Kostakopoulou K, Brickel P, Thorogood P, Feretti P. 1997. Expression of the transcription factor slug correlates with growth of the limb bud and is regulated by FGF-4 and retinoic acid. Int J Dev Biol 41:559–568.

Cooke J, Summerbell D. 1980. Cell cycle and experimental pattern duplication in the chick wing during embryonic development. Nature 287:697–701.

Fallon JF, Crosby GM. 1977. Polarizing activity in limb buds of amniotes. In: Ede DA, Hincliffe JR, Balls M, editors. Vertebrate limb and somite morphogenesis. Cambridge: Cambridge University Press.

Fisher M, Clelland AK, Bain A, Baldock R, Murphy P, Downie H, Ticke C, Davidson D, Buckland RA. 2008. Integrating technologies for comparing 3D gene expression domains in the developing chick limb. Dev Biol 317:13–23.

Fisher M, Downie H, Welten M, Delgado I, Bain A, Planzer T, Sherman A, Sang H, Baldock R, Tickle C. 2011. Comparative analysis of 3D expression patterns of transcription factor genes in the developing chick wing and digit fate maps. PLoS ONE (in press).

Francis-West PH, Robertson KE, Ede DA, Rodriguez C, Izpisua-Belmonte JC, Houston B, Burd DW, Gribbin C, Brickel PM, Tickle C. 1995. Expression of genes encoding bone morphogenetic proteins and sonic hedgehog in talpid (ta3) limb buds: their relationships in the signalling cascade involved in limb patterning. Dev Dyn 203:187–197.

Hamburger V, Hamilton H. 1951. A series of normal stages in the development of the chick embryo. J Morphol 88:49–92.

Isaac A, Rodriguez-Esteban C, Ryan A, Altabef M, Tsukui T, Patel K, Tickle C, Izpisua-Belmonte JC. 1998. Tbx genes and limb identity in chick embryo development. Development 125:1867–1875.

Katoh Y, Katoh M. 2009. Hedgehog target genes: mechanisms of carcinogenesis induced by aberrant hedgehog signaling activation. Curr Mol Med 9:873–886.

Kohler T, Prols F, Brand-Saberi B. 2005. PCNA in situ hybridisation: a novel and reliable tool for detection of

dynamic changes in proliferative activity. Histochem Cell Biol 123:315–327.

Litingtung Y, Dahn R, Li Y, Fallon JF, Chiang C. 2002. Shh and Gli3 are dispensable for limb skeleton formation but regulate digit number and identity. Nature 418:979–983.

Nieto MA. 2002. The snail superfamily of zinc-finger transcription factors. Nat Rev Mol Cell Biol 3:155–166.

Nieto MA, Patel K, Wilkinson DG. 1996. In situ hybridization analysis of chick embryos in whole mount and tissue sections. Methods Cell Biol 51:219–235.

Riddle RD, Johnson RL, Laufer E, Tabin C. 1993. Sonic hedgehog mediates the polarizing activity of the ZPA. Cell 75: 1401–1416.

Ros MA, Sefton M, Nieto MA. 1997. Slug, a zinc-finger gene previously implicated in the early patterning of the mesoderm and the neural crest, is also involved in chick limb development. Development 124:1821–1829

Saunders JW Jr, Gasseling MT. 1968. Ectoderm-mesenchymal interaction in the origins of wing symmetry. In: Fleischmajer R, Billingham RE, editors. Epithelial-mesenchymal interactions. Baltimore: Williams and Wilkins. p 19.

Sharpe J, Ahlgren U, Perry P, Hill B, Ross A, Hecksher-Sorensen J, Baldock R, Davidson D. 2002. Optical projection tomography as a tool for 3D microscopy and gene expression studies. Science 296:541–545.

te Welscher P, Zuniga A, Kuijper S, Drenth T, Goedemans HJ, Meijlink F, Zeller R. 2002. Progression of vertebrate limb development through SHH-mediated counteraction of GLI3. Science 298:827–830.

Tickle C. 2006. Making digit patterns in the vertebrate limb. Nat Rev Mol Cell Biol 7:45–53.

Towers M, Mahood R, Yin Y, Tickle C. 2008. Integration of growth and specification in chick wing digit-patterning. Nature 452:882–886.

Towers M, Fisunov G, Tickle C. 2009. Expression of E2F transcription factor family genes during chick wing development. Gene Expression Patterns 9:528–531.

Vargesson N, Clarke JD, Vincent K, Coles C, Wolpert L, Tickle C. 1997. Cell fate in the chick limb bud and relationship to gene expression. Development 124: 1909–1918.

Vokes SA, Ji H, Wong WH, McMahon AP. 2008. A genome-scale analysis of the cis-regulatory circuitry underlying sonic hedgehog-mediated patterning of the mammalian limb. Genes Dev 22: 2651–2663.

Wolpert L. 1969. Positional information and the spatial pattern of cellular formation. J Theor Biol 25:1–47.

Wyngaarden LA, Vogeli KM, Ciruna BG, Wells M, Hadjantonakis AK, Hopyan S. 2010. Oriented cell motility and division underlie early limb bud morphogenesis. Development 137:2551–2558.

Yin Y, Bangs F, Paton IR, Prescott A, James J, Davey MG, Whitley P, Genikhovich G, Technau U, Burt DW, Tickle C. 2009. The Talpid3 gene (KIAA0586) encodes a centrosomal protein that is essential for primary cilia formation. Development 136:655–664.